Research on Optimal Attitude of Large Deformation Airplane in Full-Scale Aircraft Static Test

ZHENG Jianjun[1,2*], *JIN Feng*[1], *LIU Wei*[2], *ZHANG Yiming*[3], *GUO Qiong*[2]

1. State Key Laboratory for Strength and Vibration of Mechanical Structures, School of Aerospace, Xi'an Jiaotong University, Xi'an 710049, P. R. China; 2. National Key Laboratory of Strength and Structural Integrity, Aircraft Strength Research Institute of China, Xi'an 710065, P. R. China; 3. Department of Aeronautics and Astronautics, Fudan University, Shanghai 200433, P. R. China

(Received 10 March 2025; revised 25 April 2025; accepted 25 May 2025)

Abstract: The accuracy of the full-scale aircraft static tests is greatly influenced by the aircraft attitude. This paper proposes an aircraft attitude optimization method based on the characteristics of the test. The aim is to address three typical problems of attitude control in the full-scale aircraft static tests: (1) The coupling of rigid-body displacement and elastic deformation after large deformation, (2) the difficulty of characterizing the aircraft attitude by measurable structure, and (3) the insufficient adaptability of the center of gravity reference to complex loading conditions. The methodology involves the establishment of two observation coordinate systems, a ground coordinate system and an airframe coordinate system, and two deformation states, before and after airframe deformation. A subsequent analysis of the parameter changes of these two states under different coordinate systems is then undertaken, with the objective being to identify the key parameters affecting the attitude control accuracy of large deformation aircraft. Three optimization objective functions are established according to the test loading characteristics and the purpose of the test: (1) To minimize the full-scale aircraft loading angle error, (2) to minimize the full-scale aircraft loading additional load, and (3) to minimize the full-scale aircraft loading wing root additional bending moment. The optimization calculation results are obtained by using the particle swarm optimization algorithm, and the typical full-scale aircraft static test load condition of large passenger aircraft is taken as an example. The analysis of the results demonstrates that by customizing the measurable structure of the aircraft as the observation point for the aircraft attitude, and by obtaining the translational and rotational control parameters of the observation point during the test based on the optimization objective function, the results are reasonable, and the project can be implemented and used to control the aircraft's attitude more accurately in complex force test conditions.

Key words: full-scale aircraft; static test; large deformation; position optimization; attitude control

CLC number: V216.1 **Document code:** A **Article ID:** 1005-1120(2025)03-0354-14

0 Introduction

In the testing pyramids with the building blocks approach, the full-scale aircraft static test is indispensable and of significant importance[1-4]. The main goal of the full-scale aircraft static test is to simulate, with the greatest possible accuracy, the limit states that may occur during the aircraft's operational life. It verifies whether the structure meets the specified strength requirements. Therefore, all aspects of the test should be as close to the pracitcal the limit state as possible.

The implementation of a full aircraft structural static test requires a variety of technologies, including load equivalence and application[5-13], multi-channel coordinated control[14-21], test measurement and analysis[22-26], of which the test aircraft restraint is an important supporting technology[27-30]. The role of the test restraint system is to adjust and control the

*Corresponding author, E-mail address: ylzjj_86@163.com.

How to cite this article: ZHENG Jianjun, JIN Feng, LIU Wei, et al. Research on optimal attitude of large deformation airplane in full-scale aircraft static test[J]. Transactions of Nanjing University of Aeronautics and Astronautics, 2025, 42(3): 354-367.

http://dx.doi.org/10.16356/j.1005-1120.2025.03.007

attitude of the aircraft during the test, and at the same time to feedback the amount of unevenness generated by the loading system and be balanced. In instances where minor deformation is exhibited by the aircraft, the conventional full-scale aircraft static test utilizes a six-degree-of-freedom static constraint[28-33] under the rigid-body assumption. This approach ensures the calibration of the aircraft structure within the ground coordinate system at the initial moment, obviating the necessity for any adjustments to the aircraft's attitude during the test. The employment of such a constraint method on a stiff and diminutive aircraft is conducive to the realization of the stipulated constraint objectives.

In the context of testing large-size and large-deformation aircraft, the aircraft constraint limits the displacement at the constraint point. When the structure undergoes elastic deformation, the non-constrained part deviates from its original position due to the constraint displacement limitation. To illustrate this, we consider the lateral displacement constraints on the right side of the main landing gear of an aircraft in symmetric loading conditions. In such conditions, the elastic deformation of the structure results in a lateral deviation of the main landing gear. However, the lateral constraint impedes the deformation of the main landing gear, thereby causing a deviation of the aircraft's symmetry plane from the symmetry of the ground coordinate system. The test loading direction is determined by the bearing point of the ground coordinate system and the action point of the airframe coordinate system. Deviations in the aircraft's attitude from theoretical values result in deviations in the direction of load application, thereby reducing the loading accuracy of the entire aircraft.

In response to this challenge, pioneering experimenters adopted the virtual constraint method, employing the force control method with zero load for large deformation constraint points (primarily the lateral constraint of the landing gear) to release the deformation. Since this approach effectively addressed the constraint point deformation release issue, it introduced an increased risk of constraint points failing to adhere to displacement constraints in abnormal situations, which limits its widespread adoption. Consequently, various constraint point adaptive devices have been developed for mechanical system implementation. For example, Du et al.[34] designed a ball-slide disc-type follower loading system for a certain type of rear fuselage vertical constraints; Wang et al.[27] studied the displacement compensated loading device for the displacement control of large deformation landing gear; and Liu et al.[30] designed a double-layer roller-type follower loading system for the large deformation of the main landing gear. The application of these technologies has gradually solved the main contradiction of large deformation displacement compensation for the single degree of freedom constraint in the full-scale aircraft static test.

An aircraft, as an elastic body, undergoes elastic deformation, whereby all six degrees of freedom of the body are subject to changes. Theoretically, it is imperative that all six degrees of freedom of the aircraft are meticulously controlled in order to ensure precise loading during the test. However, it is important to note that the structural components of the aircraft may deviate from their original positions during deformation. This deviation results in the reference point of the aircraft deformation, as well as the theoretical control point of the aircraft attitude during the test, becoming a theoretical problem that must be resolved.

To address this challenge, we propose an aircraft attitude control method based on the center of gravity and the six-degree-of-freedom displacement-compensated attitude control technique[29]. This method involves the control of six degrees of freedom to ensure the theoretical center of gravity of the aircraft remains constant during the test, while allowing the remaining components to deform according to the structural loading. The proposed method enhances the design of large-deformation aircraft constraints to a comprehensive elastomer cognition, thereby significantly enhancing the attitude control accuracy. However, the method also exhibits shortcomings, including the inability to measure the center of gravity, limited applicability in complex force conditions, and an absence of consideration for the

coupling relationship between the loading system and attitude change, resulting in practical implementation errors.

Based on the different configuration states before and after the deformation of a large deformation aircraft in the full-scale static test, this paper discusses the changes in the aircraft attitude and the changes in the load point caused by the structural elastic deformation and the rigid body displacement. The key parameters affecting the attitude control accuracy of the large deformation aircraft are identified by constructing two observation coordinate systems, namely the ground coordinate system and the airframe coordinate system. The two sysytems are used to compare the two deformation states before and after the deformation of the airframe, and analyze the parameter changes of the different states under them. Based on the test loading characteristics and different test purposes, three optimization objective functions are established to improve the test accuracy. The particle swarm optimization algorithm is used to obtain the optimization results of the example working condition, and in-depth analyses are carried out in terms of the reasonableness of the attitude, the feasibility of the engineering, and the accuracy compared with the traditional methods. The results show that the translational and rotational parameters of the engineering measurable control points during the test period can be obtained by the proposed method, thus supporting a better control of the aircraft attitude change. The results of the study can provide an important reference for the selection of attitude control points and attitude control of the subsequent full-aircraft static test of large deformation aircraft.

1 Position Optimization Theories

In the test process, there are two sets of coordinate systems, the laboratory ground coordinate system and the aircraft body coordinate system constructed according to the aircraft coordinate system; two coordinate bases, the loading device support force based on the ground coordinate system and the loading point based on the body coordinate system; and two deformation states, namely the initial moment of the type frame (zero-g) configuration and the deformed configuration after loading. The coupling of the elastic deformation and the rigid body displacement in the measured deformation results makes it difficult to accurately monitor the aircraft attitude, and prevents high-precision attitude control.

First, the amount of changes before and after the deformation of the aircraft is analyzed. Second, the aircraft attitude control objective, i.e. to achieve stable control of the aircraft attitude during the test, is combined with the highest theoretical loading accuracy of the whole aircraft loading point under the attitude. Then, a method based on the measurable part of the aircraft as the observation point of the airframe displacement is proposed, and an optimization algorithm is used to obtain the optimal attitude of the deformed aircraft based on the change of the force line of the loading point before and after the deformation of the aircraft. The effective control of the attitude can be achieved by linearly changing from the initial attitude to the attitude after deformation in the test.

Observation points are established at the measurable positions of the aircraft and the aircraft attitude is controlled by optimizing the change in position of the observation points before and after the deformation. Thus, the problem of the unmeasurable center of gravity is solved.

The pre-deformation zero-g configuration and the analyzed post-deformation configuration state are used as configuration benchmarks to decouple the two deformations.

Optimization is performed based on the change in configuration before and after deformation and the change in force line at the loading point to obtain optimization results before and after deformation based on specific operating conditions. Thus, more accurate universal qualitative results are achieved compared to the center of gravity benchmark.

2 Coordinate System Construction

2.1 Aircraft coordinate system construction

According to the center of gravity reference theory, in order to facilitate the displacement measure-

ment in the project implementation, the coordinate origin of the aircraft system is taken at the position of measurable points near the center of gravity. In this paper, the coordinate system origin and the reference plane $X_bO_bZ_b$ are taken in the central wing under the wall plate, as shown in Fig.1.

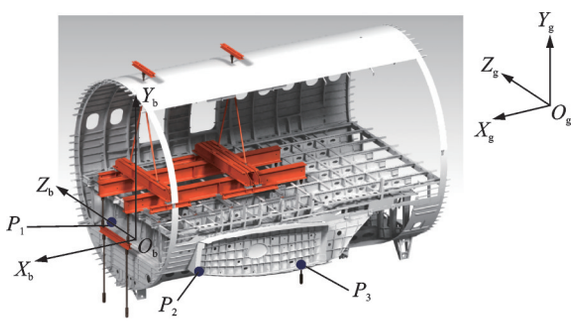

Fig.1 Schematic diagram of the origin of the coordinate system of the fuselage

The origin O_b is constructed. Two points $P_1(x_1^g, y_1^g, z_1^g)$ and $P_2(x_2^g, y_2^g, z_2^g)$ of the central wing box are selected, and the superscript g indicates the coordinates in the ground system. These two load points are in the same plane on the rear beam of the central wing. P_1 is to the left of P_2, and the two have the same x^g in the ground coordinate system when no deformation occurs, and the midpoint of P_1 and P_2 is the origin of the aircraft system O_b, namely

$$\begin{cases} x_{O_b}^g = (x_1^g + x_2^g)/2 \\ y_{O_b}^g = (y_1^g + y_2^g)/2 \\ z_{O_b}^g = (z_1^g + z_2^g)/2 \end{cases} \tag{1}$$

Z_b axis is constructed. Z_b axis is defined by two points, P_1 and P_2, and is directed from P_2 (right) to P_1 (left).

Y_b axis is constructed. P_3 is taken in front of P_1 or P_2 to form the plane $P_1P_2P_3$, with Y_b axis perpendicular to this face upwards.

X_b axis is constructed. X_b axis starts at point O_b and points to the rear of the body in the $P_1P_2P_3$ plane.

$$\begin{cases} \overrightarrow{O_bZ_b} \triangleq e_3 = \dfrac{\overrightarrow{P_2P_1}}{\overrightarrow{P_2P_1}} \\ \overrightarrow{O_bY_b} \triangleq e_2 = \dfrac{\overrightarrow{P_1P_2} \times \overrightarrow{P_2P_3}}{\left|\overrightarrow{P_1P_2} \times \overrightarrow{P_2P_3}\right|} \\ \overrightarrow{O_bX_b} \triangleq e_1 = e_3 \times e_2 \end{cases} \tag{2}$$

where (e_1, e_2, e_3) is the unit direction vector of the three coordinate axes of the aircraft coordinate system in the ground coordinate system.

The aircraft coordinate system is generated and independent of the additional position and attitude measurement points. The position and attitude of the aircraft in any given moment can thus be obtained from the three measurement points located in the center wing.

2.2 Coordinate transformation

2.2.1 Coordinate transformation matrix

In order to investigate the effect of external loads on the aircraft, the coordinates of the loading points and the positions of the loading equipment should be transferred to the aircraft coordinate system. In order to control the position of the aircraft in the test area, the loading points on the aircraft should be transferred to the ground coordinate system. Therefore, it is necessary to construct a coordinate transformation matrix.

The transformation between the aircraft coordinate system and the ground coordinate system can be divided into translation and rotation. Translation is the translation between the ground coordinate origin O_g and the aircraft coordinate origin O_b. Rotation is the rotation of the coordinate system around the coordinate origin.

Referring to the definition of flight dynamics, the coordinate system is rotated around the Z, Y, and X axes by ϑ, φ, and γ, which are defined as the pitch angle, the yaw angle, and the roll angles, respectively. The positive and the negative values of each attitude angle are defined as follows. Roll angle γ: Rotate around X axis; and the left roll is positive. Pitch angle ϑ: Rotate around the Z axis; and the low head is positive. Yaw angle φ: Rotate around Y axis; and the left deviation is positive.

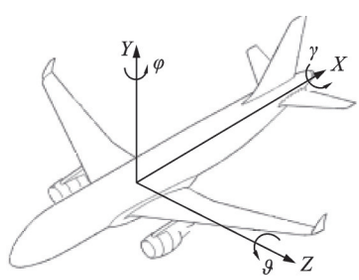

Fig.2 Schematic diagram of attitude angles

$\boldsymbol{R}_{g2b}$ is defined as the rotation matrix of the ground coordinate system rotating towards the aircraft coordinate system. $\boldsymbol{R}_{\vartheta}^{g}$, $\boldsymbol{R}_{\varphi}^{g}$, $\boldsymbol{R}_{\gamma}^{g}$ are the rotation matrices of rotating ϑ, φ, γ around Z, Y, X axes, respectively, and then rotating around the Z, Y, X axes in turn. The final rotation matrix is

$$\boldsymbol{R}_{g2b}=\boldsymbol{R}_{\vartheta}^{g}\boldsymbol{R}_{\varphi}^{g}\boldsymbol{R}_{\gamma}^{g} \tag{3}$$

Eq.(3) is the result of the multiplying of three orthogonal matrices, and also an orthogonal matrix, so that the rotation matrix of the rotation from the aircraft coordinate system to the ground coordinate system can be obtained as

$$\boldsymbol{R}_{g2b}=\boldsymbol{R}_{g2b}^{-1}=\boldsymbol{R}_{g2b}^{T} \tag{4}$$

2.2.2 Coordinate transformation of a point in space

(1) Coordinate transformation based on attitude angles

The coordinate origin O_b of the aircraft coordinate system in the ground coordinate system is defined as $O_b^g(x_{O_b}^g, y_{O_b}^g, z_{O_b}^g)$. It rotates ϑ, φ, γ around Z, Y, and X axes to obtain Z_b, Y_b, and X_b axes. Then, the aircraft coordinate system O_b-$X_bY_bZ_b$ is formed. Thus, a point $P^g(x_p^g, y_p^g, z_p^g)$ in the the coordinate O_g-$X_gY_gZ_g$ can be transformed into (x_p^b, y_p^b, z_p^b) in the aircraft coordinate system O_b-$X_bY_bZ_b$, which is described as

$$\begin{bmatrix} x_p^b \\ y_p^b \\ z_p^b \end{bmatrix}=\boldsymbol{R}_{g2b}\begin{bmatrix} x_p^g \\ y_p^g \\ z_p^g \end{bmatrix}-\begin{bmatrix} x_{O_b}^g \\ y_{O_b}^g \\ z_{O_b}^g \end{bmatrix} \tag{5}$$

(2) Coordinate transformation based on the coordinate axis vector of the aircraft coordinate system

The unit direction vector of the three coordinate axes of the aircraft coordinate system in the ground coordinate system is $\{e_1, e_2, e_3\}$, and the coordinate origin is moved from O_g to O_b. Then $\{e_1, e_2, e_3\}$ can be regarded as a set of unit orthogonal bases, and the coordinates of the space point $P^g(x_p^g, y_p^g, z_p^g)$ under the base $\{e_1, e_2, e_3\}$ can be expressed as

$$\begin{bmatrix} x_p^g \\ y_p^g \\ z_p^g \end{bmatrix}=[e_1, e_2, e_3]\begin{bmatrix} x_p^b \\ y_p^b \\ z_p^b \end{bmatrix}+\begin{bmatrix} x_{O_b}^g \\ y_{O_b}^g \\ z_{O_b}^g \end{bmatrix} \tag{6}$$

3 Optimal Attitude Modeling of Test Aircraft

In order to define the optimal position of the aircraft, it is necessary to specify the test constraints and the three states of the aircraft during the test, and to formulate the basic assumptions.

3.1 Variables and constraints involved in the test

3.1.1 Load point

The number of loading points in the test is denoted as N. The ith loading point on the fuselage is denoted as $P_{lp,i}(i=1, 2, \cdots, N)$, and its position in the ground coordinate system is labelled as $(x_{lp,i}^g, y_{lp,i}^g, z_{lp,i}^g)$, while its position in the fuselage coordinate system is labelled as $(x_{lp,i}^b, y_{lp,i}^b, z_{lp,i}^b)$.

3.1.2 Loading devices

The mounting position of the loading equipment does not change during the test. The number of loading equipment is the same as the loading point. The installation position of the ith loading equipment is marked as $P_{ld,i}(i=1, 2, \cdots, N)$, its position in the ground coordinate system is marked as $(x_{ld,i}^g, y_{ld,i}^g, z_{ld,i}^g)$, and its position in the aircraft coordinate system is marked as $(x_{ld,i}^b, y_{ld,i}^b, z_{ld,i}^b)$.

3.1.3 Test loads

The loading equipment can only use tensile or compressive force at the loading point. That is to say, the magnitude of the external load applied to the ith loading point is f_i, with the direction of this force is along the $P_{lp,i}P_{ld,i}$ continuum, and the direction vectors in the ground coordinate system and the aircraft coordinate system are noted as $\boldsymbol{n}_i^g$ and $\boldsymbol{n}_i^b$, respectively.

3.2 Three states of the airplane in the test

(1) Theoretical state

There is no deformation or attitude change of the aircraft and f_i, $\boldsymbol{n}_i^g$ and $\boldsymbol{n}_i^b$ are consistent with the design loads.

(2) Deformation state

The aircraft undergoes deformation and attitude change under load f_i. $\boldsymbol{n}_i^g$ and $\boldsymbol{n}_i^b$ change as the loading point moves.

(3) Optimized state

The aircraft deforms under the load f_i and its attitude is adjusted in a certain way to the desired state.

3.3 Basic assumption

Assumption 1 Small adjustments in attitude do not change the amount of deformation.

The elastic deformation of the aircraft is coupled to the position of the external load relative to the airframe during the loading process. The aircraft is loaded from the theoretical state to the deformed state and further adjusted to the optimized state, during which the elastic deformation of the aircraft will change slightly in response to changes in externally applied loads. The main purpose of designing the optimized state is to correct the external load to a state close to the designed load under the deformation of the airframe. This process can be regarded as a fine-tuning process, in which the deformation of the airframe is assumed to remain unchanged, which is conducive to carrying out the work of optimizing the position of the aircraft.

Assumption 2 Design loading meets force simulation needs

The static test examines the static mechanical behavior of an aircraft under certain external load, and the loading device simulates the distributed forces on the aircraft by means of a concentrated force. The loading based on the concentrated force is sufficient to simulate the real distributed force on the airframe in all kinds of working conditions. The main consideration is to adjust the fuselage attitude, so that the actual loading on the deformed airframe is as close as possible to the theoretical state of the design loading.

3.4 Positional optimization objective function establishment

The physical quantities involved in the test are organized in Table 1. The variation of physical quantities in different states is shown in Table 2.

Table 1 Physical quantities involved in the test

Physical quantity	Marking	Ground coordinate	Airframe coordinate
Load point position	$P_{\mathrm{lp},i}$	$(x^{\mathrm{g}}_{\mathrm{lp},i}, y^{\mathrm{g}}_{\mathrm{lp},i}, z^{\mathrm{g}}_{\mathrm{lp},i})$	$(x^{\mathrm{b}}_{\mathrm{lp},i}, y^{\mathrm{b}}_{\mathrm{lp},i}, z^{\mathrm{b}}_{\mathrm{lp},i})$
Load device location	$P_{\mathrm{ld},i}$	$(x^{\mathrm{g}}_{\mathrm{ld},i}, y^{\mathrm{g}}_{\mathrm{ld},i}, z^{\mathrm{g}}_{\mathrm{ld},i})$	$(x^{\mathrm{b}}_{\mathrm{ld},i}, y^{\mathrm{b}}_{\mathrm{ld},i}, z^{\mathrm{b}}_{\mathrm{ld},i})$
Load size	f_i		
Load direction		$\boldsymbol{n}^{\mathrm{g}}_i$	$\boldsymbol{n}^{\mathrm{b}}_i$

Table 2 Changes of physical quantities with state

Physical quantity	Marking	Theoretical state→ deformation state	Deformation state→ optimized state
Load point position(ground coordinate system)	$(x^{\mathrm{g}}_{\mathrm{lp},i}, y^{\mathrm{g}}_{\mathrm{lp},i}, z^{\mathrm{g}}_{\mathrm{lp},i})$	Change	Change
Load point position(airframe coordinate system)	$(x^{\mathrm{b}}_{\mathrm{lp},i}, y^{\mathrm{b}}_{\mathrm{lp},i}, z^{\mathrm{b}}_{\mathrm{lp},i})$	Change	Unchanged
Load device location(ground coordinate system)	$(x^{\mathrm{g}}_{\mathrm{ld},i}, y^{\mathrm{g}}_{\mathrm{ld},i}, z^{\mathrm{g}}_{\mathrm{ld},i})$	Unchanged	Unchanged
Load device location(airframe coordinate system)	$(x^{\mathrm{b}}_{\mathrm{ld},i}, y^{\mathrm{b}}_{\mathrm{ld},i}, z^{\mathrm{b}}_{\mathrm{ld},i})$	Change	Change
Load size	f_i	Unchanged	Unchanged
Load direction(ground coordinate system)	$\boldsymbol{n}^{\mathrm{g}}_i$	Change	Change
Load direction(airframe coordinate system)	$\boldsymbol{n}^{\mathrm{b}}_i$	Change	Change

Objective function 1 Minimize the full-scale aircraft loading pinch angle error.

Physical meanings To adjust the aircraft attitude so that the direction of the actual load applied to the airframe is the same as the direction of the theoretical load. Since the magnitude of the load remains constant, this objective can be described as the load being oriented relative to the airframe in the same direction as the design direction, or expressed as the magnitude of the component of the load in the design direction remaining the same as the design load. The external loads act relative to the airframe, so the direction of loading should be considered within the airframe.

In the body coordinate system, the load direction is defined as $\boldsymbol{n}^{\mathrm{b}}_{i,\mathrm{ll}}$ for the theoretical state, $\boldsymbol{n}^{\mathrm{b}}_{i,\mathrm{bx}}$ for

the deformed state, and $\boldsymbol{n}^{\mathrm{b}}_{i,\mathrm{yh}}$ for the optimized state. From the theoretical state to the optimized state, the deflection angle of the ith load relative to the body is

$$a_i = \arccos(\boldsymbol{n}^{\mathrm{b}}_{i,\mathrm{ll}} \cdot \boldsymbol{n}^{\mathrm{b}}_{i,\mathrm{bx}}) \tag{7}$$

The goal of aircraft attitude control can be expressed as

$$\min \sum_{i=1}^{N} a_i \quad a_i \geqslant 0 \tag{8}$$

The issue can also be described as

$$\max \sum_{i=1}^{N} (\boldsymbol{n}^{\mathrm{b}}_{i,\mathrm{ll}} \cdot \boldsymbol{n}^{\mathrm{b}}_{i,\mathrm{bx}}) \tag{9}$$

Eqs.(8,9) are equivalent formulations of the same problem.

Objective function 2 Minimize the additional load of full-scale aircraft loading

Physical meanings The deformation of the structure leads to the deviation of the actual loading direction from the theoretical loading direction, under the assumption of small deformation. The ith loading point produces an error angle α_i along the loading direction, and the angular error makes the loading point along the theoretical loading direction of the loading component is $f_i \cos\alpha_i$, and the additional load produced by the loading point along the direction perpendicular to the loading direction is $f_i \sin\alpha_i$. When α_i is small, $f_i \cos\alpha_i \approx f_i$ and $f_i \sin\alpha_i \approx f_i \cdot \alpha_i$. The load direction error mainly produces the additional load perpendicular to the loading direction, which is unacceptable in some working conditions, therefore, the objective function is constructed with the objective of minimizing the additional load as

$$\min \sum_{i=1}^{N} (f_i \cdot \sin\alpha_i) \quad \alpha_i \geqslant 0 \tag{10}$$

Objective function 3 Minimize the additional moments at the root of a full-scale loaded wing.

Physical meanings The main factor affecting the structural strength of an aircraft is the bending moment coming from the far end of the structure. Most of the wings have a thin-walled configuration, the aerodynamic loading of the wing in flight causes the aircraft to accumulate bending moment from the wing tip to the wing root, which makes the lower wing surface tensile and the upper wing surface compressive due to the thin wing surface. The bending moment transferred from the outer wing section of the wing contributes more to the internal force of the structure, and when the aircraft is deformed, the deflection curve of the wing surface of the aircraft makes the additional load of the loading point produce a larger bending moment at the wing root, which in turn affects the accuracy of the structural assessment. Therefore, if the bending moment of the additional load at the wing root can be reduced in the test, it will be beneficial to the accurate assessment of the structural strength.

The ith loading point produces the loading angle error α_i. The theoretical loading direction is $\boldsymbol{n}^{\mathrm{b}}_{i,\mathrm{ll}}$, and the loading direction is $\boldsymbol{n}^{\mathrm{b}}_{i,\mathrm{bx}}$ after deformation. The position of the loading device under the aircraft coordinate system is $\boldsymbol{r}^{\mathrm{b}}_i = (x^{\mathrm{b}}_{\mathrm{ld},i}, y^{\mathrm{b}}_{\mathrm{ld},i}, z^{\mathrm{b}}_{\mathrm{ld},i})$. Then the additional bending moment ΔM^{b}_i produced at this loading point can be described as

$$\Delta M^{\mathrm{b}}_i = M^{\mathrm{b}}_{i,\mathrm{bx}} - M^{\mathrm{b}}_{i,\mathrm{ll}} = f_i(\boldsymbol{r}^{\mathrm{b}}_{i,\mathrm{bx}} \times \boldsymbol{n}^{\mathrm{b}}_{i,\mathrm{bx}} - \boldsymbol{r}^{\mathrm{b}}_{i,\mathrm{ll}} \times \boldsymbol{n}^{\mathrm{b}}_{i,\mathrm{ll}}) \tag{11}$$

4 Optimal Aircraft Attitude Solution

4.1 Solution path

The changes of each physical quantity in Eqs.(9, 10, 11) in the process of three state transitions are examined, and summarized as the aircraft attitude optimization path, as shown in Fig.3. The objective is to obtain the aircraft attitude that makes Eqs.(9, 10, 11) take the extremes, i.e., the optimization problem for the coordinate $(x^{\mathrm{g}}_{O_{\mathrm{b}}}, y^{\mathrm{g}}_{O_{\mathrm{b}}}, z^{\mathrm{g}}_{O_{\mathrm{b}}})$ and the three attitude angles ϑ, φ, γ of the origin of the aircraft coordinate system in the ground coordinate system, which can be specifically written as

$$\min \sum_{i=1}^{N} F(\alpha_i)(x^{\mathrm{g}}_{O_{\mathrm{b}}}, y^{\mathrm{g}}_{O_{\mathrm{b}}}, z^{\mathrm{g}}_{O_{\mathrm{b}}}, \vartheta, \varphi, \gamma) \quad \alpha_i \geqslant 0 \tag{12}$$

The above problem can be converted into an optimization problem about six state quantities established on the aircraft coordinate system, describing the aircraft's position.

The particle swarm algorithm[35] is used to solve the optimal positional problem described in Eq.(12), and the algorithm flow is shown in Fig.4.

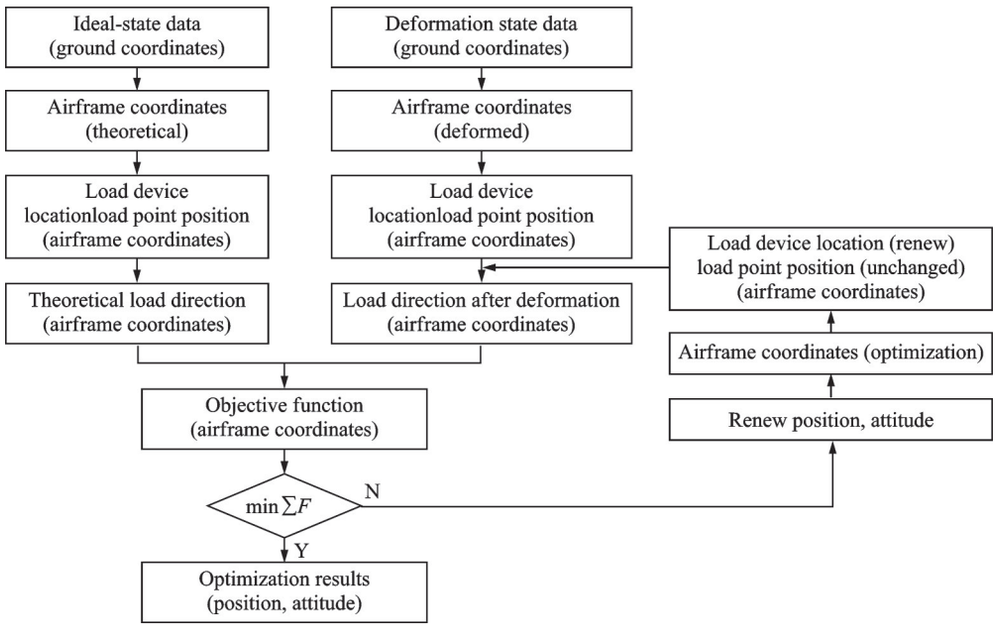

Fig.3 Position optimization path of aircraft

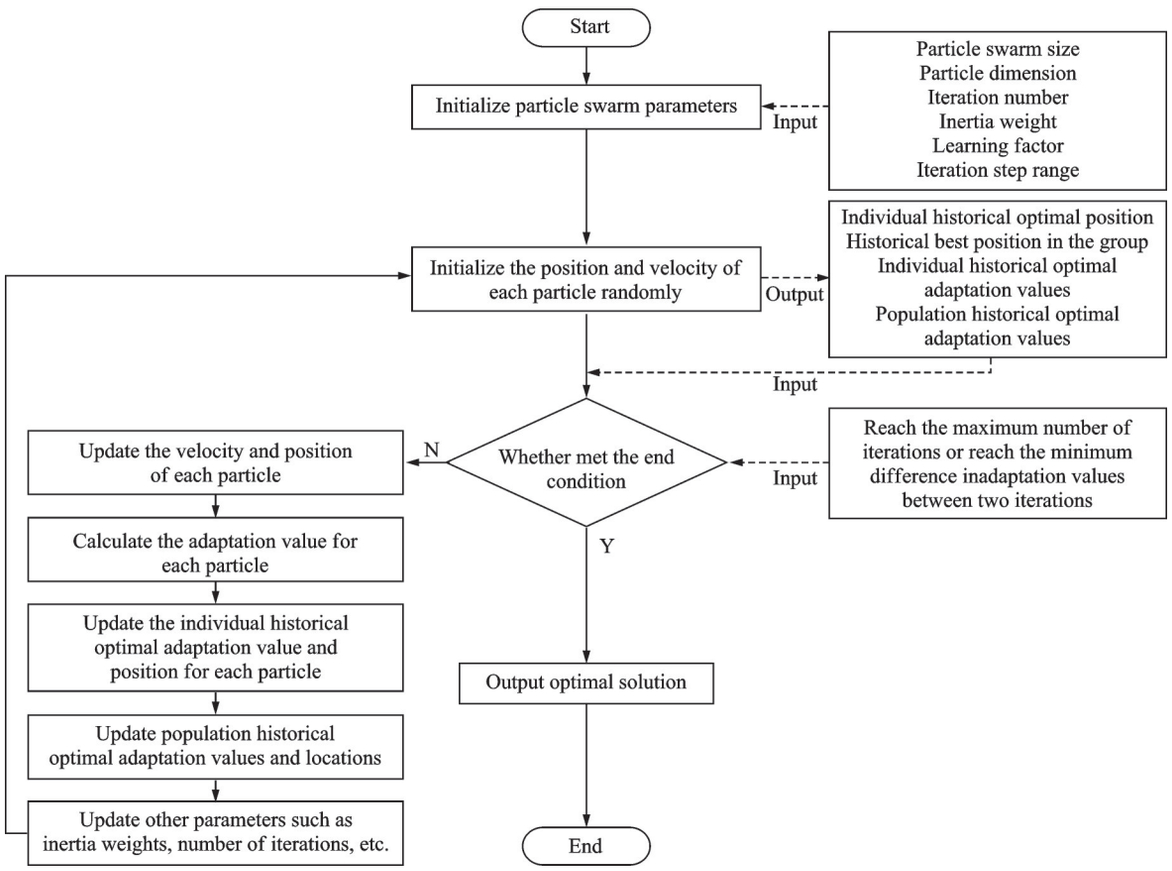

Fig.4 Flowchart of particle swarm optimization algorithm

4.2 Introduction of test cases

According to the optimization goal and test practice, three typical load conditions before and after deformation in the full-scale static test of large passenger aircraft are selected for example analysis. Case 1, the maximum vertical force landing condition, is a typical landing gear large deformation condition. The main landing gear deformation under the central wing constraint is about 200 mm in heading, 290 mm in lateral deformation, and 30 mm in verti-

cal deformation. Case 1 is mainly to study whether the optimization function can accurately obtain the positional state of the landing gear after large deformation. Case 2, stable pitch 2.5 g case, is a typical wing large deformation that is a symmetric loading case. Its symmetric lateral deformation is zero. It is to study whether the optimization function can accurately predict the position state after the wing large deformation. Case 3, the engine failure case, is a typical case of complex force and multidirectional deformation case. It is to study the optimization effect of different objective functions under the complex deformation state.

4.3 Key parameter settings and optimization results

Three points near the theoretical center of gravity of Case 1 are selected to construct the aircraft coordinate system, and the statistics of key parameters in the test are shown in Table 3. The optimization parameters of the particle swarm algorithm are shown in Table 4.

The optimization objectives, optimization results and theoretical results based on the center of gravity datum for the three case calculations are summarized in Table 5.

Table 3 Ground coordinates in different states of the airframe coordinate system for Case 1

Physical quantity	State	Coordinates/mm
$x^{\mathrm{g}}_{O_{\mathrm{b}}}, y^{\mathrm{g}}_{O_{\mathrm{b}}}, z^{\mathrm{g}}_{O_{\mathrm{b}}}$	Initial	$(2.145\,3\times10^{4}, -324, 0)$
	After deformation	$(2.139\,2\times10^{4}, -420, -5)$
$\overrightarrow{O_{\mathrm{b}}X_{\mathrm{b}}}$	Initial	$(1,0,0)$
	After deformation	$(0.999\,9, -0.013\,4, -2.196\,3\times10^{-4})$
$\overrightarrow{O_{\mathrm{b}}Y_{\mathrm{b}}}$	Initial	$(0,1,0)$
	After deformation	$(0.013\,4, 0.999\,9, 1.803\,2\times10^{-5})$
$\overrightarrow{O_{\mathrm{b}}Z_{\mathrm{b}}}$	Initial	$(0,0,1)$
	After deformation	$(2.193\,7\times10^{-4}, -2.098\,3\times10^{-5}, 1)$

Table 4 Particle swarm algorithm optimization parameters (same for three cases)

Parameter	Value		
	Lower bound	Upper bound	Initial
$x^{\mathrm{g}}_{O_{\mathrm{b}}}$	$x^{\mathrm{g}}_{O_{\mathrm{b,II}}} - 200$	$x^{\mathrm{g}}_{O_{\mathrm{b,II}}} + 200$	$x^{\mathrm{g}}_{O_{\mathrm{b}},\mathrm{bx}}$
$y^{\mathrm{g}}_{O_{\mathrm{b}}}$	$y^{\mathrm{g}}_{O_{\mathrm{b,II}}} - 200$	$y^{\mathrm{g}}_{O_{\mathrm{b,II}}} + 200$	$y^{\mathrm{g}}_{O_{\mathrm{b}},\mathrm{bx}}$
$z^{\mathrm{g}}_{O_{\mathrm{b}}}$	$z^{\mathrm{g}}_{O_{\mathrm{b,II}}} - 200$	$z^{\mathrm{g}}_{O_{\mathrm{b,II}}} + 200$	$z^{\mathrm{g}}_{O_{\mathrm{b}},\mathrm{bx}}$
Individual learning factor		1.6	
Acceleration constant		1.8	
Stock size		100	

Table 5 Summary comparison of optimization results and center of gravity benchmark

Case No.	Objective function	Control center coordinate			Attitude angle		
		X/mm	Y/mm	Z/mm	ϑ/(°)	φ/(°)	γ/(°)
1	Function 1	$2.143\,3\times10^{4}$	−418	−1	0.216	0	−0.032
2	Function 1	$2.145\,0\times10^{4}$	−368	0	0.095	0	0.006
3	Function 1	$2.146\,0\times10^{4}$	−331	6	0.013	0	−0.027
3	Function 2	$2.145\,3\times10^{4}$	−324	0	0	0	0
3	Function 3	$2.145\,3\times10^{4}$	−331	7	0.008	0.009	0.002
Traditional method	Barycenter based	$2.145\,3\times10^{4}$	−300	0	0	0	0

5 Result Analysis

5.1 Result reasonableness analysis

In the maximum vertical force landing condition, the case is characterized by complete symmetry in the loading to ensure that the lateral deformation of the fuselage is negligible. In this scenario, the bending moment experienced by the rear fuselage is notably larger, and the main landing gear is subjected to significant stress. Subjected to the effect of the maximum vertical force, which leads to a large downward deformation of the rear fuselage, re-

sulting in a large pitch angle of the aircraft fuselage, which needs to be corrected during the test. A comparison of the optimization results in Table 5 reveals that the lateral deformation of Case 1 is −1 mm, the pitch angle is 0.21°, and the yaw angle is 0°, which are consistent with the actual situation. Additionally, the optimization results also have a roll angle of −0.032°, which is a smaller value, and this may be attributed to a calculation error, and can be disregarded.

Case 2 is a stabilized pitch 2.5 g case, as well as a typical, completely symmetric loaded wing large deformation case. Thus, the lateral deformation of the symmetric plane is 0, and the roll and yaw angle under symmetric loading should be 0. For the pitch angle, a small amount of change is evident in this case due to the torsion of the central wing structure. However, the pitch angle should be lower than that of the maximum vertical force landing case. A comparison of the optimization results for Case 2, as presented in Table 5, reveals a lateral displacement of 0, a pitch angle of 0.095°, which is in accordance with the expectation, and a yaw angle of 0°, which is also in accordance with the expectation. However, a small amount of computational error is observed in the roll angle as 0.006°, though this is negligible and can be disregarded in engineering.

Case 3 presents a complex force condition, involving the fuselage lateral bending and torsion. Consequently, the center of the aircraft coordinate system should exhibit a slight degree of lateral displacement, and the three degrees of freedom of rotation should each have a small value. This is due to the relatively low value of the load. Therefore, the absolute value of each of these degrees of freedom should be less than that observed in Case 1 and Case 2.

A comparison of the optimization results of the three objective functions for Case 3 in Table 5 reveals that objective functions 1 and 3 align with this characteristic, while the optimization result of objective function 2 approaches 0. This is attributable to the fact that objective function 2 solely considers the effect of vertical loading deformation on lateral additional load, disregarding the error associated with vertical loading itself. Consequently, this results in an error in the optimization result. With regard to the rotational degree of freedom, the optimization results of objective function 1 and objective function 3 are minimal, as expected, while the optimization results of objective function 2 are all 0. This is because this objective function only considers the effect of loading deformation on the lateral load, indicating its insensitivity to changes in the rotational degree of freedom. However, it can be disregarded in engineering due to its minimal value.

A thorough examination of the vertical direction optimization results for the three cases reveals that all three optimization functions exhibit vertical displacement changes. This phenomenon can be attributed to the fact that the vertical displacement of the aircraft exerts an influence on the loading angle in the actual loading. In the context of the actual loading, the central wing undergoes a downward bend subsequent to the application of the bending moment, resulting in the observation point deforming in a downward direction. The optimization results align with the characteristics of the deformation.

In summary, the optimization results of the three optimization objective functions are generally consistent with the actual load and deformation characteristics. Among them, objective function 1 is more sensitive to the calculation, with a small amount of calculation error in two optimization conditions, and objective function 3 is not sensitive to the optimization of rotational degrees of freedom.

5.2 Implement ability analysis

As demonstrated by the optimization results of Case 1 and Case 2, the full-scale aircraft finite element model employs the same constraint site and incorporates forced displacement, subsequently calculating the constraint point displacement compensation values, as outlined in Table 6. In Table 6, the

Table 6 Optimized landing gear displacement

Case No.	Location	X_g/mm	Y_g/mm	Z_g/mm
1	Front landing gear	13.75	72.84	7.42
	Left main landing gear	208.81	292.53	−16.85
	Right main landing gear	209.04	288.06	28.11
2	Front landing gear	16.95	34.30	0.56
	Left main landing gear	28.73	140.94	32.62
	Right main landing gear	28.31	141.54	−36.57

displacement of each constraint point is within the permissible range and is engineering implementable. A comparison of Case 1 and Case 2 reveals that the former exhibits significant elastic deformation due to the main landing gear being subjected to a substantial ground reaction force. In contrast, the latter main landing gear experiences no load and only undergoes a coordinated deformation of the structure. Consequently, the compensation value of Case 1 is expected to be considerably larger than that of Case 2. The calculation results presented in Table 6 are consistent with the actual deformation characteristics.

An examination of the Z-displacement compensation amount in Table 6 reveals an error of approximately 7 mm in the overall lateral displacement of Case 1. However, given that the test case is a symmetry case, it should be a deformed symmetry. The reason for the observed outcome is that the optimization result of Case 1 has a roll angle of $-0.032\,4^{\circ}$, and the constraint points are located beneath the fuselage construction level. The overall lateral deviation of the constraint points can be attributed to the full roll of the aircraft. The presence of the roll in the calculation result may be attributed to the coordinate deviation of the loading point and the calculation error.

5.3 Precision analysis of optimization results

As demonstrated in Table 5, which presents the results of Case 1 and Case 2, the optimization method and the center of gravity benchmark method demonstrate consistency in terms of the lateral displacement and the yaw angle. However, the optimization method exhibits a minor advantage in terms of the pitch and the roll angle, which is better in line with the actual state according to the analysis in section 5.1. This is because the difference in the amount of values is minimal, indicating that a more accurate attitude control target can be obtained in both symmetric loading cases, and that the optimization method can obtain more accurate results of the pitch angle.

Examining Case 3, the lateral translation result of using the optimized objective function 1 and objective function 3 is not 0, which is better in line with the actual loading characteristics and is consistent with the results of the finite element analysis of the full-scale aircraft. The lateral translation displacement of the optimized objective function 2 is 0, indicating that the function is not sensitive to the lateral displacement. The rotational degrees of freedom of objective function 1 and objective function 3 are not 0, while those of objective function 2 and the center of gravity reference method are 0. According to the previous analysis of this case, the three rotational degrees of freedom should have a small amount, which indicates that the objective functions 1 and 3 have a more accurate rotational degrees of freedom optimization effect. The result of objective function 2 is consistent with that of the center of gravity benchmark method. It fails to provide better results.

In summary, for symmetric load cases, both the center of gravity benchmark and the optimization method can obtain engineering acceptable results, and the optimization objective functions 1 and 3 are more realistic for pitch optimization. For complex force cases, the optimization objective functions 1 and 3 can obtain better optimization results compared with the center of gravity benchmark, and the optimization objective function 2 results are consistent with the center of gravity benchmark, which cannot achieve high accuracy of attitude optimization.

6 Conclusions

Aiming at the problem of the optimal theoretical control center for the full-scale aircraft static test of large deformation aircraft, this paper proposes the optimal position analysis method based on the test characteristics. The main innovations are as follows.

(1) A position optimization method based on test characteristics is proposed to solve the problem of the difficulty in determining the aircraft attitude control target due to the existence of two reference coordinate systems and two deformation states in the process of the full-aircraft static test of a large-deformation aircraft.

(2) The objectives of minimum error of the full-aircraft loading angles, the minimum additional load of the full-aircraft loading, and the minimum additional moment of the full-aircraft loading wing

root, are established, and the physical significance is interpreted. The mathematical model is provided for the optimization calculations. A comparative analysis is conducted, which demonstrates that the theoretical attitude of the full-aircraft static test utilizing the optimization algorithm is both reasonable and implementable in engineering. Furthermore, it is determined that the optimization objective functions 1 and 3 can serve to guide a more accurate control of the attitude of the test aircraft.

(3) In consideration of the three most typical full-aircraft loading conditions, including the full-scale aircraft stable pitch, the maximum vertical force landing and the yaw maneuver as illustrative cases, the optimal attitude analysis results of the test are obtained by employing the particle swarm optimization algorithm. The optimization analysis has facilitated the progress of aircraft attitude from qualitative conclusions to quantitative evaluation.

References

[1] ZHANG Zhaobin, LI Mingqiang, LI Jian. Research on comprehensive planning and implementation for full-scale static test of large transporter[J]. Aeronautical Science & Technology, 2015, 26(10): 25-27. (in Chinese)

[2] LIN Jianhong. The historical developments and trendencies of building block approach and testing pyramid[J]. Advances in Aeronautical Science and Engineering, 2023, 14(5): 8-18. (in Chinese)

[3] WANG Yupeng, PEI Lianjie, LI Qiulong, et al. Full-scale aircraft strength test technology of next generation fighter[J]. Acta Aeronautica et Astronautica Sinica, 2020, 41(6): 523482. (in Chinese)

[4] ZHENG Jianjun, TANG Jiyun, WANG Binwen. Static test technology for C919 full-scale aircraft structure[J]. Acta Aeronautica et Astronautica Sinica, 2019, 40(1): 210-221. (in Chinese)

[5] ZHENG Jianjun, WANG Mengmeng, ZHANG Lei, et al. Rigid loading accelerates full-scale aircraft fatigue test[C]//Proceedings of the 31st ICAF Symposium. Delft, The Netherlands:[s.n.], 2023.

[6] ZHANG Tuo, SONG Pengfei, YIN Wei, et al. Follow-up loading technology for lift structure with spatial complex movement[J]. Acta Aeronautica et Astronautica Sinica, 2022, 43(6): 506-518. (in Chinese)

[7] GUO Qiong, LIU Wei, PEI Lianjie, et al. Static and fatigue test technology for full-scale composite fuselage barrels[J]. Acta Aeronautica et Astronautica Sinica, 2022, 43(6): 415-424. (in Chinese)

[8] REN Peng, DU Xing. Application of large curvature curved surface structure loading technology in aircraft strength test[J]. Science Technology and Engineering, 2021, 21(10): 4255-4259. (in Chinese)

[9] ZHANG Tuo, DU Xing, WANG Xintao, et al. Research and application of electric servo loading technology for landing gear fatigue test[J]. Machine Tool & Hydraulics, 2020, 48(10): 70-75. (in Chinese)

[10] WANG Xintao, DU Xing. Research on differential loading method for aircraft structural strength test[J]. Machine Tool & Hydraulics, 2020, 48(10): 80-83. (in Chinese)

[11] WANG Xintao, DU Xing. Emergency load limited system for aircraft structural strength test[J]. Acta Aeronautica et Astronautica Sinica, 2020, 41(2): 220-230. (in Chinese)

[12] MA Jiming, WANG Fei, YANG Guangwu, et al. Design and analysis of one type of pulse filter for hydraulic system[J]. Acta Aeronautica et Astronautica Sinica, 2019, 40(11): 290-298. (in Chinese)

[13] LIU Wei, TENG Qing, LIU Bing. Double-deck bi-directional loading technology based on airliner cabin floor structure[J]. Acta Aeronautica et Astronautica Sinica, 2018, 39(5): 136-143. (in Chinese)

[14] ZHAO Hongwei, DUAN Shihui, YANG Shengchun, et al. Influence of friction force on output force of asymmetrical cylinder controlled by servo valve[J]. Hydraulics & Pneumatics, 2015(2): 59-61, 78 (in Chinese).

[15] ZHAO Hongwei, FENG Jianmin, HAN Tao, et al. Closed-loop cross-compensation control for multi-channel structural fatigue testing system[J]. Control Engineering of China, 2021, 28(2): 395-400. (in Chinese)

[16] SHIM J Y. Evaluating the accuracy of load application for static structural testing of aerospace flight vehicles[J]. International Journal of Aeronautical and Space Sciences, 2020, 21(1): 133-152.

[17] GAO C H, ZHENG S T, CONG D C, et al. Modeling and control of the CSCEC multi-function testing system[J]. Journal of Earthquake Engineering, 2018, 22(2): 257-280.

[18] KWEDER J, PANTHER C, SMITH J. Applications of circulation control, yesterday and today[J]. International Journal of Engineering, 2010, 4(5): 411-429.

[19] CHEN Y, WICKRAMASINGHE V, ZIMCIK D. Active control of a hybrid actuation system for aircraft vertical fin buffet load alleviation[J]. The Aeronautical Journal, 2006, 110(1107): 315-326.

[20] CHEN Y, VIRESH W, ZIMCIK D. Development

and verification of real-time controllers for the F/A-18 vertical fin buffet load alleviation[C]//Proceedings of Smart Structures and Materials 2006: Smart Structures and Integrated Systems. San Diego, USA: SPIE, 2006: 304-315.

[21] JUNG J K, LEE K B, YANG M S, et al. A study on the test load simulation technique for T-50 full scale durability test[J]. Journal of the Korean Society for Aeronautical & Space Sciences, 2004, 32(3): 82-87.

[22] TIAN Kuo, SUN Zhiyong, LI Zengcong. High-precision digital twin method for structural static test monitoring[J]. Acta Aeronautica et Astronautica Sinica, 2024, 45(7): 429134. (in Chinese)

[23] KOLMAN E M, KURULYUK D V, LIMONIN M V. Actual methods of full-scale metal-composite aircraft structures static testing with the use of information systems[J]. Journal of Physics: Conference Series, 2021, 1990(1): 012012.

[24] LI S J, ZHANG G G, WANG J. Civil aircraft health management research based on big data and deep learning technologies[C]//Proceedings of 2017 IEEE International Conference on Prognostics and Health Management (ICPHM). Dallas, USA: IEEE, 2017: 154-159.

[25] CHEN X H, FAN H T, PEI J L, et al. Real time monitoring and forecasting of full scale aircraft static test[J]. Tsinghua Science & Technology, 2009, 14: 38-42.

[26] LIU Yalong, WANG Shengnan, LIU Haifeng, et al. Development of test data tracking, analyzing and processing system for aircraft structural strength based on MSC/PATRAN platform[J]. Acta Aeronautica et Astronautica Sinica, 2007, 28(1): 84-89. (in Chinese)

[27] WANG Xintao, XIA Long, LIU Xingke. Research on landing gear displacement compensation loading technology of the whole structural test[J]. Machine Tool & Hydraulics, 2021, 49(8): 55-59. (in Chinese)

[28] WANG Mengmeng, LIU Bing, WANG Gaoli. Research on load modification method of large aircraft landing gear[J]. Chinese Journal of Applied Mechanics, 2021, 38(2): 708-714. (in Chinese)

[29] ZHENG Jianjun, WANG Binwen, ZHU Lingang, et al. Research on attitude control and constraint system design of full-scale aircraft static test based on barycenter[C]//Proceedings of the 32rd Congress of the International Council of the Aeronautical Sciences. Shanghai, China:[s.n.], 2003.

[30] LIU Wei, ZHENG Jianjun. Self-adaptable loading technique for main landing gears in structural test of large airliner[J]. Aeronautical Science & Technology, 2020, 31(12): 42-47. (in Chinese)

[31] WANG Xintao, DU Xing. Research and application of strength test support system of multi-wheel and multi-strut landing gears aircraft[J]. Machine Tool & Hydraulics, 2020, 48(9): 95-98. (in Chinese)

[32] WANG Gaoli, TANG Jiyun. Error analysis & optimization for constraint point load of full scale aircraft test[J]. Engineering & Test, 2014, 54(2): 42-46. (in Chinese)

[33] LIU Quanliang, YIN Wei, XIA Feng. The determination of support scheme for aircraft static strength verification test[J]. Aeronautical Science & Technology, 2012, 23(5): 32-35. (in Chinese)

[34] DU Xing, FENG Jianmin, HE Qian. Self-adaptable loading technique for undercarriage in full scale aircraft structure test[J]. Science Technology and Engineering, 2017, 17(2): 288-292. (in Chinese)

[35] ZHANG Y D, WANG S H, JI G L. A comprehensive survey on particle swarm optimization algorithm and its applications[J]. Mathematical Problems in Engineering, 2015, 2015: 931256.

Acknowledgement This work was supported in part by the National Specialized Research Project (No.XXZ3-XX21-3).

Author

The first/corresponding author Mr. **ZHENG Jianjun**, senior engineer, is a Class I Technical Expert at the China Aeronautical Establishment (CAE). He has long been engaged in research on full-scale aircraft structural static/fatigue strength testing and related technologies. He has led or participated in numerous critical national military/civil aircraft projects, including the C919, MA700, and J-20, conducting full-scale aircraft structural static strength and fatigue strength tests.

Author contributions Mr. **ZHENG Jianjun** conducted the conceptualization, designed the methodology, and wrote the draft. Prof. **JIN Feng** contributed to the conceptualization and the design of the methodology. Mr. **LIU Wei** conducted resource collection and validation. Dr. **ZHANG Yiming** conducted formal analysis and software development. Ms. **GUO Qiong** conducted visualization and helped the draft in terms of reviewing and editing. All authors commented on the manuscript draft and approved the submission.

Competing interests The authors declare no competing interests.

(Executive Editor: ZHANG Bei)

大变形飞机全机静力试验最优位姿研究

郑建军[1,2],金 峰[1],刘 玮[2],张易明[3],郭 琼[2]

(1. 西安交通大学航天航空学院机械结构强度与振动国家重点实验室,西安 710049,中国; 2. 中国飞机强度研究所强度与结构完整性全国重点实验室,西安 710065,中国; 3. 复旦大学航空航天系,上海 200433,中国)

摘要:全尺寸飞机结构静力试验的精度受飞机姿态影响显著。本文基于试验特点,提出了一种飞机姿态优化方法,旨在解决全尺寸飞机静力试验中姿态控制的3个典型问题:(1)大变形后飞机刚体位移与飞机结构弹性变形的耦合问题;(2)飞机姿态难以通过可测结构表征的问题;(3)重心参考点对复杂加载工况适应性不足的问题。本方法通过建立两个观测坐标系(地面坐标系和机体坐标系)及两个变形状态(机体变形前和变形后),随后分析这两个状态在不同坐标系下的参数变化,目标在于识别影响大变形飞机姿态控制精度的关键参数。根据试验加载特性和试验目的,建立了3个优化目标函数:(1)全机加载载荷角度误差最小;(2)全机加载附加载荷最小;(3)全机加载机翼附加弯矩最小。以大型客机全机静力试验典型载荷工况为例,利用粒子群优化算法获得了优化计算结果。结果表明,通过选定飞机的可测部位作为飞机姿态观测点,基于优化目标函数获得试验中该观测点的平动和转动控制参数,结果合理、项目可实施,且能指导在复杂受力试验工况下更精确地控制飞机姿态。

关键词:全尺寸飞机;静力试验;大变形;位姿优化;姿态控制